
A Bayesian model of acquisition and clearance of bacterial colonization

Marko Järvenpää^{1,2}, Mohamad R. Abdul Sater², Georgia K. Lagoudas^{3,4}, Paul C. Blainey^{3,4}, Loren G. Miller⁵, James A. McKinnell^{5,6}, Susan S. Huang⁷, Yonatan H. Grad^{2,*}, Pekka Marttinen^{1,*}

¹Aalto University ²Harvard TH Chan School of Public Health ³MIT ⁴Broad Institute, MIT and Harvard ⁵LA Biomedical Research Institute, Harbor-UCLA Medical Center ⁶LA County Department of Public Health, Acute Communicable Disease Control Unit ⁷University of California, Irvine School of Medicine (*equal contribution)

Abstract

Bacterial populations that colonize a host play important roles in host health, including serving as a reservoir that transmits to other hosts and from which invasive strains emerge, thus emphasizing the importance of understanding rates of acquisition and clearance of colonizing populations. Studies of colonization dynamics have been based on assessment of whether serial samples represent a single population or distinct colonization events. A common solution to estimate acquisition and clearance rates is to use a fixed genetic distance threshold. However, this approach is often inadequate to account for the diversity of the underlying within-host evolving population, the time intervals between consecutive measurements, and the uncertainty in the estimated acquisition and clearance rates. Here, we summarize recently submitted work [14] and present a Bayesian model that provides probabilities of whether two strains should be considered the same, allowing to determine bacterial clearance and acquisition from genomes sampled over time. We explicitly model the within-host variation using population genetic simulation, and the inference is done by combining information from multiple data sources by using a combination of Approximate Bayesian Computation (ABC) and Markov Chain Monte Carlo (MCMC). We use the method to analyse a collection of methicillin resistant *Staphylococcus aureus* (MRSA) isolates.

1 Introduction

Colonizing bacterial populations are often the source of infecting strains and transmission to new hosts [23, 24, 12, 2, 7], making it important to understand the dynamics of these populations and the factors that contribute to persistent colonization and to the success or failure of clinical decolonization protocols. The study of colonization dynamics is based on inferring whether bacteria from samples collected over time represent the same population or distinct colonization events, thereby permitting calculation of rates of acquisition and clearance [6, 16]. Whole genome sequencing has provided a detailed measure of genetic distance between isolates, which can then be used to infer the relationship between them [9, 22, 19, 21]. While to date most studies have used genetic distance thresholds as the basis for determining the relationship between isolates [19, 9], in this text we improve on these heuristic strategies and present a robust and accurate fully probabilistic model that provides probabilities of whether two strains should be considered the same.

The Bayesian statistical framework allows to combine information from multiple data sources. In this approach, a prior distribution is updated using the laws of probability into a posterior distribution in the light of the observations, and this can be repeated multiple times with different data sets

[10, 18]. Approximate Bayesian computation (ABC) is particularly useful with population genetic models, where the likelihood function may be difficult to specify explicitly, but simulating the model is feasible [4, 15]. ABC has recently been introduced in bacterial population genetics [3, 17, 13, 8]. Here, we present a Bayesian model for determining whether two genomes should be considered the same strain, enabling a strategy grounded in population genetics to make inferences about acquisition and clearance from data of closely related genomes. Benefits of this approach include: rigorous quantification of uncertainty, explicit statement of modeling assumptions (open for criticism and further development), and straightforward utilization of multiple data sources. We demonstrate these benefits by analyzing a large collection longitudinally collected MRSA genomes, obtained through a clinical trial (Project CLEAR) to evaluate the effectiveness of an MRSA decolonization protocol [1].

2 Data sources

One input data item from [1] for our model consists of a pair of genomes that are of the same sequence type (ST), sampled from the same individual at two consecutive time points (or possibly with an intervening time point with no samples or a sample of a different ST). All the sampled genomes are from nasal swabs. Each of these pairs of consecutive genomes is summarized in terms of two quantities: the distance between the genomes $d_i \in \{0, 1, 2, \dots\}$ and the difference between their sampling times $t_i > 0$ (see Fig 4). Hence, the observed data, which we denote by D , can be written as consisting of pairs (d_i, t_i) , $i = 1, \dots, N$.

As external data we use measurements from eight patients colonised with MSSA [12], comprising nasal swabs from two time points for each patient, such that the acquisition is known to have happened approximately just before the first swab. Multiple genomes were sequenced from each sample, and the distributions of pairwise distances between the genomes provide snapshots to the within-host variability at the two time points for each individual, and these distance distributions are used as additional data. The data set also contains observations from an additional 13 patients from [11], denoted by letters from A to M in [12]. For these patients, distance distributions from only one time point are available. The data from the 8 + 13 patients is jointly denoted by D_0 .

3 Outline of the model and the inference algorithms

Overview of the proposed approach, including data sets, models, and methods for inference, is outlined in Fig 1 and discussed in the following in more detail. An essential part of our approach is a population genetic simulation which allows us to model the within-host variation, and hence make probabilistic statements of the plausibilities of the 'same strain' vs. 'different strain' cases. For this purpose, we adopt the common Wright-Fisher (W-F) simulation model, see e.g. [20], with a constant mutation rate μ and effective population size n_{eff} , which are estimated from the data. The simulation is started with all genomes being the same, which corresponds to a biological scenario according to which a colonization begins with a single isolate multiplying rapidly until reaching the maximum 'capacity', followed by slow diversification of the population.

Let (s_{i1}, s_{i2}) denote a pair of genomes with distance d_i , sampled from a patient at two consecutive time points with time difference t_i . Here we present a model, i.e., a probability distribution $p_S(d_i | t_i, n_{\text{eff}}, \mu)$, which tells what kind of distances we should expect if the genomes are from the same strain. We model d_i as $d_i = d_{i1} + d_{i2}$ where we have defined $d_{i1} = \text{dist}(s_{i1}, s_{i*})$ and $d_{i2} = \text{dist}(s_{i*}, s_{i2})$, where $\text{dist}(\cdot, \cdot)$ is a distance function that tells the number of mutations between its arguments, and s_{i*} is the unique ancestor of s_{i2} that was present in the host when s_{i1} was sampled, and which has descended within the host from the same genome as s_{i1} (see Fig 2A). The probability distribution of d_{i1} which is denoted by $p_{\text{sim}}(d_{i1} | n_{\text{eff}}, \mu)$, and which is not available analytically and does not depend on t_i , represents the within-host variation at a single time point, and we define it implicitly as

$$p_{\text{sim}}(d_{i1} | \mu, n_{\text{eff}}) = \text{WF-simulator}(d_{i1} | \mu, n_{\text{eff}}). \quad (1)$$

The distribution of d_{i2} is assumed to be $d_{i2} | \mu, t_i \sim \text{Poisson}(d_{i2} | \mu t_i)$, that is, mutations are assumed to occur according to a Poisson process with the rate parameter μ .

Model p_D represents the case that the genomes s_{i1} and s_{i2} are from different strains, which we define to mean that their most recent common ancestor (MRCA), denoted by s_{iA} , resided outside the host. The time between s_{iA} and s_{i1} is denoted by t_{0i} (see Fig 2B). Under model p_D , we assume that the

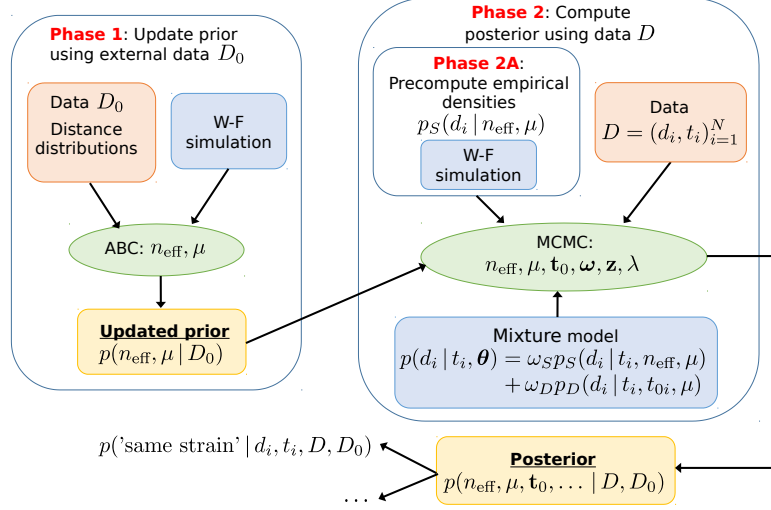


Figure 1: Overview of the modeling and data fitting steps.

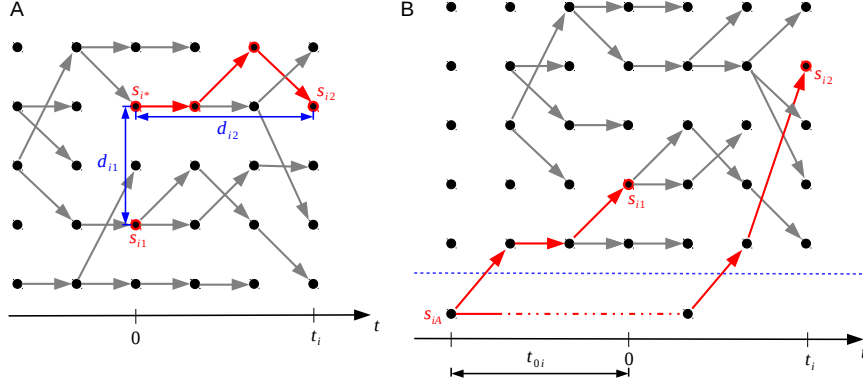


Figure 2: Outline of the 'same strain' and 'different strain' models. Model p_D on the panel A represents the situation where the genomes denoted by s_{i1} and s_{i2} are of the same strain. Model p_S on the panel B shows the case where these genomes are of different strains.

distribution of the distance d_i is

$$p_D(d_i | \mu, t_i, t_{0i}) = \text{Poisson}(d_i | \mu(2t_{0i} + t_i)), \quad (2)$$

where the values of t_{0i} are unknown and will be estimated.

With the two alternative models for the distance, we write the full model, which assumes that each distance observation is distributed according to

$$p(d_i | t_i, \theta) = \omega_S p_S(d_i | t_i, n_{\text{eff}}, \mu) + \omega_D p_D(d_i | t_i, t_{0i}, \mu), \quad i = 1, \dots, N, \quad (3)$$

where θ denotes jointly all the parameters of the models, i.e., $\theta = (n_{\text{eff}}, \mu, \omega_S, \omega_D, t_{01}, \dots, t_{0N})$. The parameter ω_S represents the proportion of pairs from the same strain and ω_D is the proportion of pairs from different strains, such that $\omega_S + \omega_D = 1$.

Because the values of t_{0i} in Eq 2, denoting the times to the MRCA in case the sequences are different strains, are unknown, we model them as random variables and use the hierarchical prior distribution

$$t_{0i} | k, \lambda \sim \text{Gamma}(k, \lambda), i = 1, \dots, N \quad \text{and} \quad \lambda \sim \text{Gamma}(\alpha, \beta). \quad (4)$$

The parameter λ is thus shared between different t_{0i} which allows us to learn about its distribution. We set $k = 5$, $\alpha = 2.5$, and $\beta = 1600$, which approximately correspond to the mean and

Table 1: Posterior mean and 95% credible interval (CI) for the 'global' parameters of the mixture model. The estimated 'nuisance' parameters t_{0i} and class labels z_i are not shown here.

parameter	mean	95% CI
n_{eff}	1700	[1300, 2200]
$\mu (\times 10^4)$	7.6	[6.0, 9.2]
ω_S	0.87	[0.83, 0.91]
ω_D	0.13	[0.09, 0.17]
$\lambda (\times 10^5)$	7.3	[5.8, 9.0]

Table 2: Posterior means of different patterns of consecutive samples and the estimated acquisition and clearance rates (mean, 95% CI in parenthesis, 'str' refers to strain).

event	expected number	
ST A, str X \rightarrow ST A, str X	231	
ST A, str X \rightarrow ST A, str Y	34	
ST A \rightarrow ST B	45	
ST A, str X \rightarrow \emptyset	104	
$\emptyset \rightarrow$ ST A, str X	21	
rate parameter	post. estimate	baseline
acquisition rate r_{acq}	0.18(0.17, 0.19)	0.16
clearance rate r_{clear}	0.25(0.24, 0.25)	0.24

standard deviation of 5800 and 8400 generations, respectively. This weakly informative prior reflects the notion that different strains diverged on average approximately a year ago, but with a large variance. Furthermore, we set $\omega = (\omega_S, \omega_D) \sim \text{Dir}(1, 1)$. As a prior for (n_{eff}, μ) , we use $n_{\text{eff}} \sim \mathcal{U}(\{20, 21, \dots, 10000\})$, $\mu \sim \mathcal{U}([a_\mu, b_\mu])$ with $a_\mu = 0.00005$ and $b_\mu = 0.005$ mutations per genome per generation. We then use ABC inference, extensive W-F forward simulations and the external data D_0 to obtain (approximate) posterior $p(n_{\text{eff}}, \mu | D_0)$ which is further used as a prior for the mixture model.

As in e.g. [5], we introduce hidden labels (denoted jointly by \mathbf{z}) which specify the component which generated each observation d_i . This allows to derive a Gibbs sampling algorithm for the posterior of the augmented model. To make the inference fast, we use various additional tricks, e.g. we reparametrize the model and block some parameters to obtain better mixing of the MCMC. Since the densities in Eq. 1 are available only implicitly, we estimate them empirically with additional W-F simulations. Due to lack of space we omit further details of the resulting MCMC algorithm.

4 Experiments and conclusion

The estimated 'global' parameters of the mixture model given the observed data sets D and D_0 described in Section 2 are presented in Table 1. We have also investigated the efficiency of the MCMC method using simulated data and some of the results are shown in the appendix. We computed acquisition and clearance rates using our model fitted to the data, and compared those to the ones obtained with the common strategy of using a fixed distance threshold of 40 ('baseline' case). These results are shown in Table 2 along with some statistics on the expected number of different events in the data. We see that the threshold-based estimates are relatively similar to, and only slightly smaller than the estimates from our model. Importantly, while being consistent with the previous results, our model bypasses the task of heuristically choosing a single threshold and adds uncertainty estimates around the point estimates, crucial for drawing rigorous conclusions.

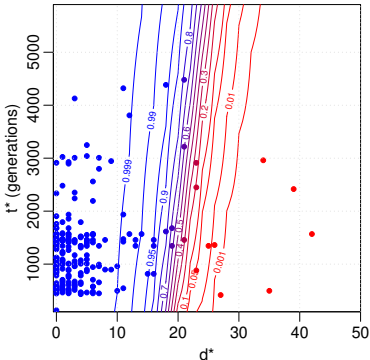


Figure 3: Same strain probability of a new measurement with distance d^* and time interval t^* .

Fig 3 shows the posterior distribution for the probability of the same strain case for a (hypothetical future) observation with distance d^* and time difference t^* . Blue colour in the figure denotes high probability of the same strain. The corresponding 50% classification curve is (almost) a straight line with a steep positive slope. This is as expected since the same strain model can explain a greater number of mutations when more time has passed. Approximately 20 mutations draws the line between the same strain and different strains cases within the time difference up to 6000 generations (approximately one year).

To summarize, we presented a model for the analysis of clearance and acquisition of bacterial colonization, which, unlike previous approaches, does not rely on a heuristic fixed distance threshold to determine whether genomes observed at different times points are from the same or different acquisition. Fully probabilistic, the model automatically provides uncertainty es-

timates for all relevant quantities and takes into account the variation in the time intervals between pairs of consecutive samples. As future work, we will extend the model to cover genomes sampled from multiple body sites.

Acknowledgments

We acknowledge the computational resources provided by Aalto Science-IT project.

References

- [1] Agency for Healthcare Research and Quality (AHRQ). Project clear (changing lives by eradicating antibiotic resistance) trial. <https://clinicaltrials.gov/ct2/show/NCT01209234>. Last accessed 08-23-2018, 2018.
- [2] M. T. Alam, T. D. Read, R. A. Petit, S. Boyle-Vavra, L. G. Miller, S. J. Eells, R. S. Daum, and M. Z. David. Transmission and microevolution of *usa300* *mrsa* in us households: evidence from whole-genome sequencing. *MBio*, 6(2):e00054–15, 2015.
- [3] M. A. Ansari and X. Didelot. Inference of the properties of the recombination process from whole bacterial genomes. *Genetics*, 196(1):253–265, 2014.
- [4] M. A. Beaumont, W. Zhang, and D. J. Balding. Approximate Bayesian computation in population genetics. *Genetics*, 162(4):2025–2035, 2002.
- [5] C. M. Bishop. *Pattern Recognition and Machine Learning (Information Science and Statistics)*. Springer-Verlag New York, Inc., 2006.
- [6] M. S. Calderwood. Editorial commentary: Duration of colonization with methicillin-resistant staphylococcus aureus: A question with many answers. *Clinical infectious diseases: an official publication of the Infectious Diseases Society of America*, 60(10):1497, 2015.
- [7] F. Coll, E. M. Harrison, M. S. Toleman, S. Reuter, K. E. Raven, B. Blane, B. Palmer, A. R. M. Kappeler, N. M. Brown, M. E. Török, et al. Longitudinal genomic surveillance of *mrsa* in the uk reveals transmission patterns in hospitals and the community. *Science Translational Medicine*, 9(413):eaak9745, 2017.
- [8] N. De Maio and D. J. Wilson. The bacterial sequential markov coalescent. *Genetics*, 206(1):333–343, 2017.
- [9] X. Didelot, A. S. Walker, T. E. Peto, D. W. Crook, and D. J. Wilson. Within-host evolution of bacterial pathogens. *Nature Reviews Microbiology*, 14(3):150, 2016.
- [10] A. Gelman, J. B. Carlin, H. S. Stern, D. B. Dunson, A. Vehtari, and D. B. Rubin. *Bayesian data analysis*. Chapman & Hall/CRC Texts in Statistical Science, third edition, 2013.
- [11] T. Golubchik, E. M. Batty, R. R. Miller, H. Farr, B. C. Young, H. Larner-Svensson, R. Fung, H. Godwin, K. Knox, A. Votintseva, et al. Within-host evolution of staphylococcus aureus during asymptomatic carriage. *PLoS One*, 8(5):e61319, 2013.
- [12] N. Gordon, B. Pichon, T. Golubchik, D. Wilson, J. Paul, D. Blanc, K. Cole, J. Collins, N. Cortes, M. Cubbon, et al. Whole-genome sequencing reveals the contribution of long-term carriers in staphylococcus aureus outbreak investigation. *Journal of Clinical Microbiology*, 55(7):2188–2197, 2017.
- [13] M. Järvenpää, M. U. Gutmann, A. Vehtari, and P. Martinen. Gaussian process modeling in approximate bayesian computation to estimate horizontal gene transfer in bacteria. *Annals of Applied Statistics*, 2018. to appear, preprint arXiv:1610.06462.
- [14] M. Järvenpää, M. R. A. Sater, G. K. Lagoudas, P. C. Blainey, L. G. Miller, J. A. McKinnell, S. S. Huang, Y. H. Grad, and P. Martinen. A Bayesian model of acquisition and clearance of bacterial colonization incorporating within-host variation. <https://www.biorxiv.org/content/early/2018/09/27/429464>, 2018.
- [15] J. Lintusaari, M. U. Gutmann, R. Dutta, S. Kaski, and J. Corander. Fundamentals and Recent Developments in Approximate Bayesian Computation. *Systematic biology*, 66(1):e66–e82, 2017.

- [16] R. R. Miller, A. S. Walker, H. Godwin, R. Fung, A. Votintseva, R. Bowden, D. Mant, T. E. Peto, D. W. Crook, and K. Knox. Dynamics of acquisition and loss of carriage of staphylococcus aureus strains in the community: the effect of clonal complex. *Journal of Infection*, 68(5):426–439, 2014.
- [17] E. Numminen, L. Cheng, M. Gyllenberg, and J. Corander. Estimating the transmission dynamics of streptococcus pneumoniae from strain prevalence data. *Biometrics*, 69(3):748–757, 2013.
- [18] A. O’Hagan and J. Forster. *Advanced Theory of Statistics, Bayesian inference*. Arnold, London, UK, second edition, 2004.
- [19] J. R. Price, K. Cole, A. Bexley, V. Kostiou, D. W. Eyre, T. Golubchik, D. J. Wilson, D. W. Crook, A. S. Walker, T. E. Peto, et al. Transmission of staphylococcus aureus between health-care workers, the environment, and patients in an intensive care unit: a longitudinal cohort study based on whole-genome sequencing. *The Lancet Infectious Diseases*, 17(2):207–214, 2017.
- [20] M. H. Schierup and C. Wiuf. The coalescent of bacterial populations. *Bacterial Population Genetics in Infectious Disease*, pages 1–18, 2010.
- [21] A.-C. Uhlemann, J. Dordel, J. R. Knox, K. E. Raven, J. Parkhill, M. T. Holden, S. J. Peacock, and F. D. Lowy. Molecular tracing of the emergence, diversification, and transmission of s. aureus sequence type 8 in a new york community. *Proceedings of the National Academy of Sciences*, 111(18):6738–6743, 2014.
- [22] C. J. Worby, M. Lipsitch, and W. P. Hanage. Within-host bacterial diversity hinders accurate reconstruction of transmission networks from genomic distance data. *PLoS Computational Biology*, 10(3):e1003549, 2014.
- [23] B. C. Young, T. Golubchik, E. M. Batty, R. Fung, H. Larner-Svensson, A. A. Votintseva, R. R. Miller, H. Godwin, K. Knox, R. G. Everitt, et al. Evolutionary dynamics of staphylococcus aureus during progression from carriage to disease. *Proceedings of the National Academy of Sciences*, 109(12):4550–4555, 2012.
- [24] B. C. Young, C.-H. Wu, N. C. Gordon, K. Cole, J. R. Price, E. Liu, A. E. Sheppard, S. Perera, J. Charlesworth, T. Golubchik, et al. Severe infections emerge from commensal bacteria by adaptive evolution. *elife*, 6:e30637, 2017.

Appendix

Visualisation of the MRSA data D

An example of a typical individual-level longitudinally sampled data set (denoted by D in the main text) from a study population also used in our analysis is shown in Fig 4: each ‘row’ represents a patient, x-axis is time, and dots are the genomes sampled at multiple time points. Dot color refers to different, easily distinguishable, sequence types (ST). The coloured number between two consecutive samples reflects the distance between the genomes, and we see that even within the same ST the distances may vary considerably, and, therefore, determining whether the changes can be explained by within-host evolution only, is challenging. Intuitively, if two genomes are very similar, we interpret this as a single strain colonizing the host. On the other hand, two very different genomes, even if the same ST, are interpreted as two different strains, obtained either jointly or separately as two acquisitions.

Results with simulated data

To empirically investigate the identifiability of the mixture model parameters and the correctness and consistency of our MCMC algorithm under the assumption that the model is specified correctly, we first fit the mixture model to simulated data. We generate artificial data from the mixture model with parameter values similar to the estimates for the observed data D from the next section. Specifically, we choose $n_{\text{eff}} = 2, 137$, $\mu = 0.0011$, $\omega_S = 0.8$, $\lambda = 0.0001$ and we repeat the analysis with various data sizes N . We use otherwise similar priors as for the real data except that, for simplicity, instead of using the prior obtained from the ABC inference, we use a uniform prior. We then fit the mixture model to the simulated data sets to investigate if the true parameters can be recovered (identifiability) and whether the posterior becomes concentrated around their true values when the amount of data increases (consistency).

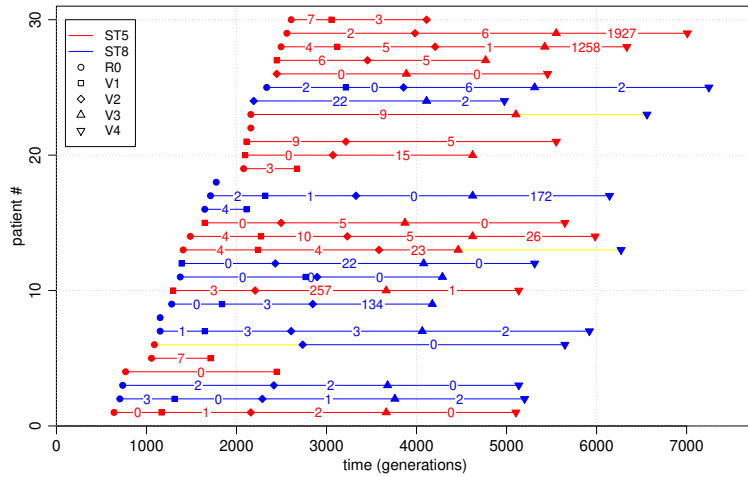


Figure 4: Illustration of a subset of the data used in the study. Each row corresponds to one patient and only the first 30 patients are shown. R0 is the initial hospital visit and V1, V2 etc. are the further visits. Red colour refers to ST5 and blue to ST8 and the coloured numbers are the amount of mutations d_i . Yellow colour highlights the cases where the ST changes from ST 5 to ST 8.

Results are illustrated in Fig 5. The first three panels show the estimated posterior distributions for parameters (n_{eff}, μ) of the mixture model using simulated data of different sizes N . The light grey dots denote the grid point locations needed for numerical computations.

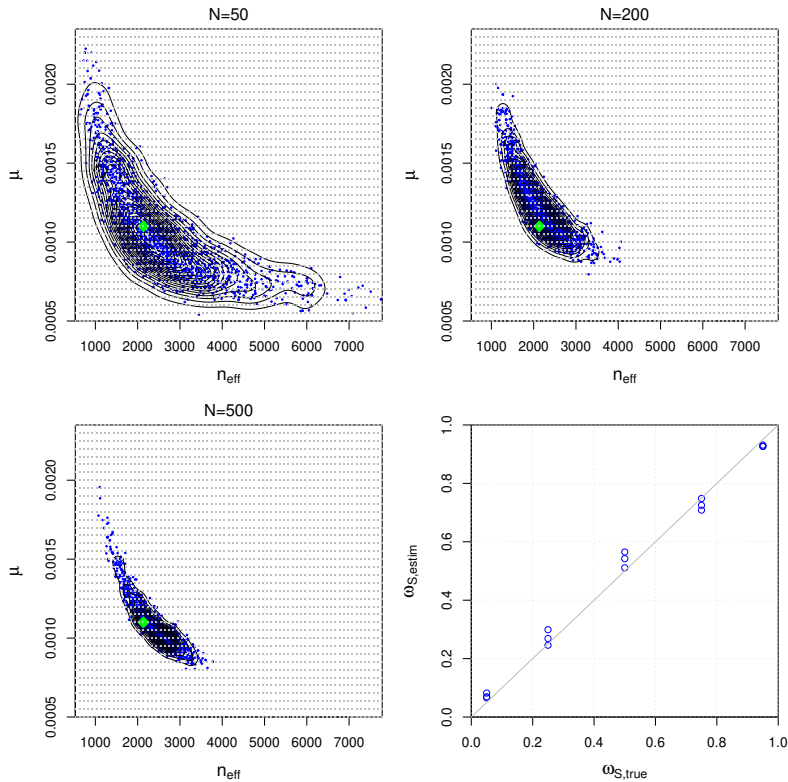


Figure 5: Illustration of the accuracy and consistency with synthetic data.

We see that the (marginal) posterior of (n_{eff}, μ) is concentrated around the true parameter value that was used to generate the data (green diamond in the figure). Also, despite the fact that the number of parameters increases as a function of data size N (because each data point (d_i, t_i) has its own class indicator z_i and time to the most recent common ancestor t_{0i} parameter), the marginal posterior distribution of (n_{eff}, μ) can be identified and appears to converge to the true value as N increases.

The panel in the lower right corner of Fig 5 shows results from an additional simulation experiment where the mixture model is fitted to data generated with different values for the ω_S parameter, which represents the proportion of pairs that are from the same strain. Other than that and the fact that we fixed $N = 150$, the experimental design is the same as above. The results show that the estimated ω_S values generally agree well with the true values.